Wavefield separation via PCA and deep learning in the Local Angle Domain

Liron Itan, Yuval Serfaty, David Chase and Zvi Koren, Paradigm Geophysical*

Summary

We present a novel method for decomposing different geometrical characteristics of seismic imaged data using principle component analysis (PCA) applied to directional (dip/azimuth) gathers, and then performing deep learning (convolutional neural network) for automatic classification interpretation. The subsurface geometrical objects to be classified are reflectors (continuous structural surfaces) and different types of diffractors (discontinuous objects such as small-scale fractures and faults). Our preliminary results show superiority over other methods involved in geometrical transformation (e.g., Radon) and specular/diffraction weighted stacks.

Introduction

Specular/diffraction imaging has proven to be an attractive approach for providing high-resolution subsurface images containing different types and scales of discontinuous geometrical objects. Specular/diffraction imaging in the prestack time domain has been intensively studied (e.g., Khaidukov et al., 2004, Shtivelman and Keydar, 2005, Fomel et al., 2006, Berkovitch et al., 2009 and others). Kozlov et al., (2004) presented diffraction imaging in depth using a "side wave" Kirchhoff-type migration, where the migration aperture was tapered to filter out the specular energy. Moser and Howard (2008) presented the implementation of diffraction imaging in depth for 2D models, providing a comprehensive review of and insight into the potential of diffraction waves to obtain high-resolution images of small-scale discontinuous subsurface objects. Reshef and Landa (2009) showed the application of diffraction energy within dip gathers for high-resolution velocity analysis, especially in areas containing discontinuous objects or along irregular interfaces. For real depth domain 3D subsurface models, Koren et al., (2008), Koren and Ravve (2010), and in particular, Koren and Ravve (2011) described a novel imaging method which is based on the ability to decompose the full recorded seismic wavefield into continuous full-azimuth directivity components in situ at the subsurface image points. The proposed method follows the concept of imaging and analysis in the local angle domain (LAD). Further implementations and enhancements of this method have been presented by Inozemtsev et al., (2013), Kowalski et al., (2014), Konyushenko et al., (2014), Inozemtsev et al., (2015), Chase and Koren (2015), and Benfield et al., (2016).

The work presented in this abstract is a continuation of the above studies, where we show the power of first applying PCA on directional (subsurface dip/azimuth of the local normals) gathers (e.g., Koren and Ravve, 2011) and then performing convolutional neural network training and prediction (Rumelhart et al., 1986 and Krizhevsky et al., 2012) for obtaining high-resolution, noise-free, continuous structural surfaces and discontinuous objects, like faults and fracture systems. We demonstrate our method on seimic data acquired in the Eagle Ford shale.

Method

The proposed method follows the concept of imaging and analysis in the Local Angle Domain (LAD). PCA measures are performed in local windows around individual depth points and all directivity bins within the directional LAD gathers. The output is the principle directivities, i.e., the wavefield patterns of each distinguished geometrical object, such as continuous structural surfaces (reflectors), faults and fractures, point diffractors, and systematic and random noise, all decomposed into different images. An additional advantage of PCA is its inherent compression, as all of the relevant information presented is in a significantly smaller dataset than the number of directivities in the directional LAD gathers.

The next stage involves training the convolutional neural network with many examples of different geometrical features. Convolutional neural networks consist of multiple layers, where each layer contains a set of learnable filters with a small visual field of the input image. During the traning process, each filter is convolved across the width and height of the input image, computing the dot product between the entries of the filter and the input, and producing an activation map of that filter. As a result, the network learns filters that activate when it detects a specific type of feature at some spatial position in the input.

In this research we have used "off the shelf" network, where all but the last of its neural layers have been trained on a variety of images, not necessarily seismic. We have trained the last neural layer with 2700 examples, generated from five different surveys and classified into five distinguishable geometrical features, as shown in Figure 1. The classification features include reflectors, faults, a specific type of point diffractor (an intersection of two reflective planes), coherent migration "smiles", and random noise.

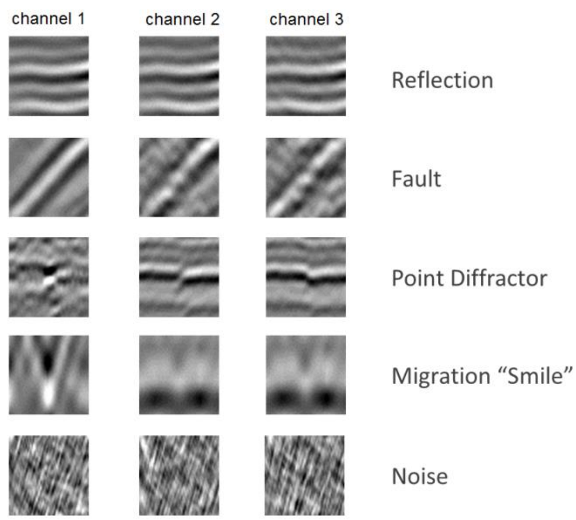

Figure 1: Channel 1 - PCA applied on each direction for aperture of 10°. Channel 2 - PCA applied on each direction for aperture of 20°. Channel 3 - PCA applied on each direction for aperture of 40°.

In order to increase classification accuracy, due to the relatively small data set used, we have inserted each feature into three channels of the same image, where the difference for each channel is the directional aperture that was extracted from the directional LAD gathers. For example, a point diffractor principle component on a directivity aperture of 10° appears as a single, high amplitude point. The principle component on a directivity aperture of 40° appears as the intersection of two shifted horizons. This operation increases the credibility of the network learning process.

Examples

The Eagle Ford shale is shown here as a test case for the trained convolutional neural network. Figure 2 shows a section of a directional LAD gather stack without any processing. PCAs of the directional LAD gathers were given to the neural network for classification.

Figure 3 shows the same section as in Figure 2, where the image was constructed by principle components that were classified as “Noise” by the convolutional neural network.

Figure 4 shows the same section as in Figure 2, where the image was constructed by principle components that were classified as “Reflectors” by the convolutional neural network. The result in Figure 4 clearly shows the noise reduction and enhancement of the reflector’s continuity.

Figure 5 shows the same image as in Figure 4, overlaid with windows containing principle components that were classified as “Fault” (in red color) and “Point Diffractor” (in green color). The image in those windows was constructed by the appropriate principle components, i.e., the fault lines and point diffractors are extracted with high resolution.

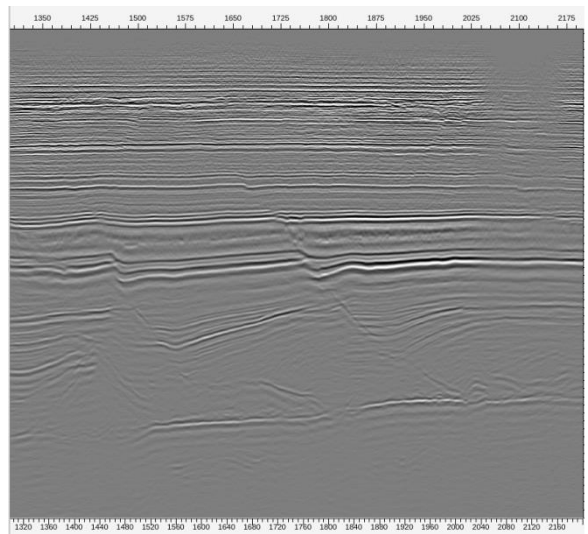

Figure 2: A section of the Eagle Ford shale, generated by a directional LAD gather stack without any processing.

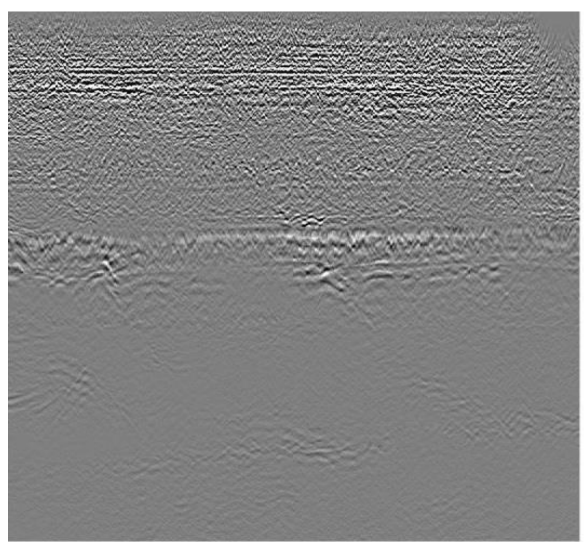

Figure 3: PCAs of the Eagle Ford section that were classified as “Noise” by the convolution neural network.

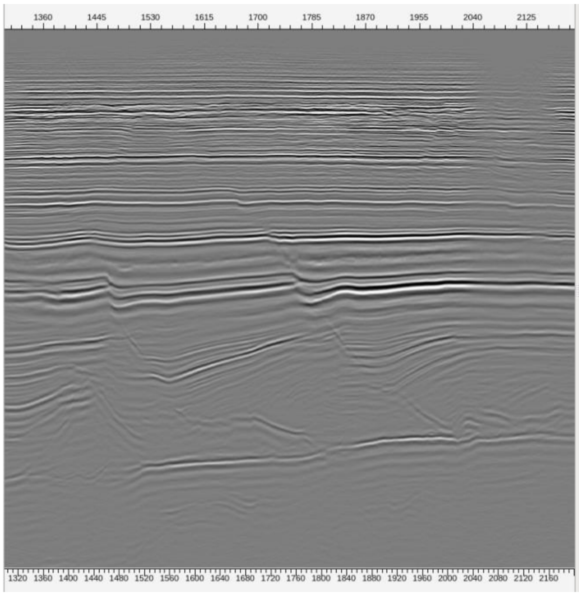

Figure 4: PCAs of the Eagle Ford section that were classified as “Reflectors” by the convolution neural network.

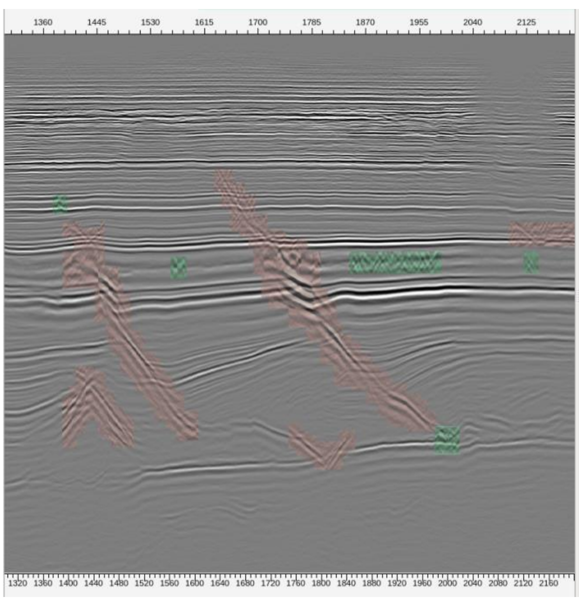

Figure 5: Overlaying the reflector image, PCAs that were classified as “Fault” appear in red colored windows and PCAs that were classified as “Point Diffractor” appear in green colored windows.

Conclusions

Seismic data acquired in the Eagle Ford Shale is used to demonstrate the applicability of PCA and deep learning applied to prestack data, in order to generate high-resolution seismic images that allow a more confident interpretation of continuous structural surfaces and small scale discontinuous objects. This approach shows great promise in identifying subsurface structural features with high accuracy, low cost (no processing preparation was needed) and simple yet scalable implementation - higher accuracy can be achieved by extensive classification in the training process. Training can be performed over more hidden layers and more iterations.

Acknowledgements

We would like to thank Paradigm for authorizing us to publish this abstract.

EDITED REFERENCES

Note: This reference list is a copyedited version of the reference list submitted by the author. Reference lists for the 2017 SEG Technical Program Expanded Abstracts have been copyedited so that references provided with the online metadata for each paper will achieve a high degree of linking to cited sources that appear on the Web.

REFERENCES

Benfield, N., A. Guise, and D. Chase, 2016, Diffraction imaging – a tool to reduce exploration and development risk: First Break, **34**, 57–63.

Berkovitch, A., I. Belfer, Y. Hassin, and E. Landa, 2009, Diffraction imaging by multifocusing: Geophysics, **74**, no. 6, WCA75–WCA81, https://doi.org/10.1190/1.3198210.

Chase, D., and Z. Koren, 2015, 5D local angle domain gathers as an ideal representation for directivity driven imaging: 77th Annual International Conference and Exhibition, EAGE, Extended Abstracts, WS12-B02, http://doi.org/10.3997/2214-4609.201413550.

Fomel, S., E. Landa, and M. T. Taner, 2006, Post-stack velocity analysis by separation and imaging of seismic diffractions: 76th Annual International Meeting, SEG, Expanded Abstracts, 2559–2563.

Inozemtsev, A., S. Nicolaevich, I. Viktorovich, A. Galkin, R. Vasilyevich, and Z. Koren, 2013, Applying full–azimuth angle domain pre-stack migration and AVAZ inversion to study fractures in carbonate reservoirs in the Russian Middle Volga region: First Break, **31**, 79–83.

Inozemtsev, A., Z. Koren, and G. Zapprikaspiygeofizika, 2015, Noise suppression and multiple attenuation using full-azimuth angle domain imaging: case studies: First Break, **33**, 81–86.

Khaidukov, V., E. Landa, and T. J. Moser, 2004, Diffraction imaging by focusing-defocusing: An outlook on seismic su-perresolution: Geophysics, **69**, 1478–1490, https://doi.org/10.1190/1.1836821.

Konyushenko, A., V. Shumilyak, V. Solgan, A. Inozemtsev, V. Solovyev, and Z. Koren, 2014, Using full-azimuth imaging and inversion in a Belarus salt dome tectonic regime to analyze fracturing in Upper Devonian intersalt and subsalt carbonate reservoirs: First Break, **32**, 81–88.

Koren, Z., and I. Ravve, 2010, Specular/diffraction imaging by full azimuth subsurface angle domain decomposition: 80th Annual International Meeting, SEG, Expanded Abstracts, https://doi.org/10.1190/1.3513526.

Koren, Z., and I. Ravve, 2011a, Full-azimuth subsurface angle domain wavefield decomposition and imaging Part I: Directional and reflection image gathers: Geophysics, **76**, no. 1, S1–S13, https://doi.org/10.1190/1.3511352.

Koren, Z., and I. Ravve, 2011b, Full-azimuth subsurface angle domain wavefield decomposition and imaging: Part 2—Local angle domain: Geophysics, **76**, no. 2, S51–S64, https://doi.org/10.1190/1.3549742.

Koren, Z., I. Ravve, E. Ragoza, A. Bartana, and D. Kosloff, 2008, Full-azimuth angle domain imaging: 78th Annual International Meeting, SEG, Expanded Abstracts, 2221–2225, https://doi.org/10.1190/1.3059327.

Kowalski, H., P. Godlewski, W. Kobusinski, W. Makarewicz, M. Podolak, A. Nowicka, Z. Mikolajewski, D. Chase, R. Dafni, A. Canning, and Z. Koren, 2014, Imaging and

characterization of a shale reservoir onshore Poland, using full-azimuth seismic depth imaging: First Break, **32,** 101–109.
Kozlov, E., N. Baransky, E. Korolev, A. Antonenko, and E. Koshchuk, 2004, Imaging scattering objects masked by specular reflections: 74th Annual International Meeting, SEG, Expanded Abstracts, 1131–1134, https://doi.org/10.1190/1.1851082.
Krizhevsky, A., I. Sutskever, and G. E. Hinton, 2012, Imagenet classification with deep convolutional neural networks, *in* Advances in neural information processing systems, **25**, 1106–1114.
Moser, T. J., and C. B. Howard, 2008, Diffraction imaging in depth: Geophysical Prospecting, **56**, 627–641, http://doi.org/10.1111/j.1365-2478.2007.00718.x.
Reshef, M., N. Lipzer, and E. Landa, 2009, Interval velocity analysis in complex areas - azimuth considerations: 71st Annual International Conference and Exhibition, EAGE, Extended Abstracts, U010, http://doi.org/10.3997/2214-4609.201400368.
Rumelhart, D. E., G. E. Hinton, and R. J. Williams, 1986, Learning internal representations by error propagation, *in* D. E. Rumelhart, and J. L. McClelland, eds., Parallel distributed processing: explorations in the microstructure of cognition: MIT Press, **1**, 318–362.
Shtivelman, V., and S. Keydar, 2005, Imaging shallow subsurface inhomogeneities by 3D multipath diffraction summation: First Break, **23**, 39–42, https://doi.org/10.3997/1365-2397.2005001.